GSA Data Repository 2013223

Model details, simplifications and sensitivity tests

The reaction-transport model was developed in R - an open source statistical computing environment (R Development Core Team). Code was developed using 'ReacTran', a package of functions, routines and solvers for reactive-transport modeling (Soetaert and Meysman, 2009). In addition, packages 'seacarb' and 'marelec' are used to calculate initial carbonate speciation, equilibrium constants and diffusion coefficients of chemical species under the specified physical and chemical conditions (Soetaert et al., 2010; Lavigne and Gattuso, 2012). The task of carrying out batches of multiple model runs, for example, to test the sensitivity of results to a particular parameter, can made more efficient using parallel computing. The 'multicore' package was used to divide tasks between processor cores (Urbanek, 2009).

The reaction-transport model finds a numerical solution to a set of 13-coupled partial differential equations describing the temporal change in distribution of [CO_2], [HCO_3^-], [CO_3^{2-}], [$^{13}CO_2$], [$^{13}HCO_3^-$], [$^{13}CO_3^{2-}$], [H^+], [OH^-], [SO_4^{2-}], [CH_4], [H_2S], [HS^-], and [Ca^{2+}] in a 1D porous sedimentary profile subject to diffusion and advection (transport), and chemical reactions (summarized in Table DR 3 and detailed below). Exchange with ocean water, assumed to behave as an infinite reservoir and represented by upper boundary conditions (Table DR 4), occurs by diffusion only. Advection and diffusion rates are calculated based on the physical parameters defined in Table DR 4.

Explicit kinetics of all chemical reactions of the carbonate system are included in the model (Table DR 3) using the approach of Zeebe and Wolf-Gladrow, (2001).

No rate constants are available for the dissociation of hydrogen sulfide, therefore, following the approach of Aloisi (2008), this reaction is considered to be very fast, with a rate constant of 1×10^{10} $kg.mmol^{-1}.a^{-1}$ ascribed to the protonation of HS^-. The reverse reaction rate constant can then be calculated using the hydrogen sulfide dissociation constant (Millero, 1995).

AOM in seeps is mediated by microbial consortia (Hoehler et al., 1994; Boetius et al., 2000), therefore a Michaelis–Menten expression is used to describe response of AOM rates to changing methane and sulfate concentration:

$$R_{AOM} = v_{\max}\left(\frac{[CH_4]}{[K_{CH_4} + [CH_4]]}\right)\left(\frac{[SO_4^{2-}]}{K_{SO_4}[SO_4^{2-}]}\right), \qquad (1)$$

where R_{AOM} is the rate of anaerobic methane oxidation, v_{max} is the maximum AOM rate, and K_{CH4} and K_{SO4} are the half-saturation constants of methane and sulfate, respectively.

This expression mimics the effect of enzyme saturation, which places upper limits on reaction rates. The concentration of reactants at which enzyme saturation occurs is related to half-saturation constants. Laboratory studies indicate a half-saturation constant of ~0.5 mM for sulfate (K_{SO4}), with K_{CH4} having values in the mM range (Wegener and Boetius, 2009). Therefore K_{SO4} and K_{CH4} are set at 0.5 and 1mM, respectively. Sensitivity tests show that the exact choice of half-saturation constants is not critical - the influence on isotope composition of pore fluids is minor.

Carbonate precipitation rates depend on the saturation state of pore waters with respect to calcium carbonate (Ω), given by:

$$\Omega_{CaCO_3} = \frac{[Ca^{2+}][CO_3^{2-}]}{K_{sp}} \qquad (2)$$

K_{sp} is the solubility product of aragonite. Ω_{CaCO3} is linked to carbonate precipitation rates by the expression:

$$R_{carbprec} = k_{carbprec}(\Omega_{CaCO_3} - 1)^n \qquad (3)$$

$K_{carbprec}$ is the kinetic constant for carbonate precipitation and $n = 3$, accounting for the non-linear dependence of precipitation rate on saturation state.

Organic matter (OM) flux: Models of modern seeps usually take fluxes of OM to the sediment/water interface and subsequent burial into account because bacterial sulfate reduction of OM consumes sulfate. This reaction typically reduces the sulfate available for AOM and depresses the SMTZ (Regnier et al., 2011). Reactive OM may also fuel methanogenesis when oxidants are exhausted, boosting the supply of methane for AOM (Regnier et al., 2011). The OM flux was assumed to be zero in our model because we

wish to optimize AOM, even at low $[SO_4^-]_{SW}$. At low $[SO_4^-]_{SW}$, methane is not the limiting factor on AOM rates in our simulations, it is set to seawater saturation at the lower model boundary, so additional generation in the sediment profile is not expected to impact AOM rates in a significant way.

Sensitivity test of other parameters*:* Seeps form in a variety of settings encompassing a range of physical and chemical conditions. Table DR 5 shows the influence of changing various parameters (temperature, pressure, upper boundary pH, porosity, methane concentration at the lower boundary and diffusive boundary layer thickness) between natural extremes (while holding others at baseline values), on $\delta^{13}C$ of carbonate precipitates, SMTZ depth and the integrated AOM rate. $\delta^{13}C_{PDB}$ variability is <1 ‰, confirming our assertion that $[SO_4^-]_{SW}$, DIC concentrations and isotopic composition of methane subject to AOM are the main controls on $\delta^{13}C_{PDB}$ of seep carbonates.

Influence of other electron acceptors on AOM: Recent research has shown that bio-available, solid Fe^{3+} phases (oxides and oxy-hydroxides), may fuel AOM in addition to sulfate (e.g. Beal et al., 2009). The potential impact of Fe^{3+} based AOM on the temporal distribution of seep deposits was not considered in the present paper however, because unlike sulfate, sedimentary recharge of Fe^{3+} by diffusion cannot take place, severely limiting the extent of AOM. Furthermore, even in situations where Fe^{3+} is in plentiful supply (like the lab experiments of Beal et al., 2009), AOM using Fe^{3+} proceeds at ~15% of the rate when sulfate is utilized. We also note that in the Proterozoic and Paleozoic, reducing oceanic conditions would also limit the flux of reactive Fe(III) phases reaching the seafloor. These factors severely limit the localized production of carbonate cements that are typically dominant mineral phase in ancient seep sediments.

FIGURES

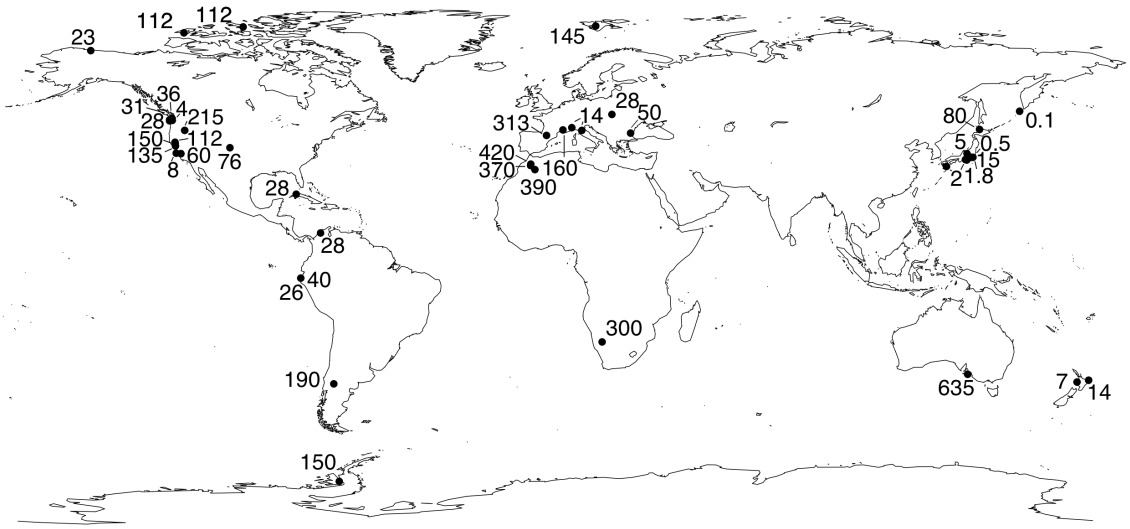

Figure DR1. Map showing the location and age (Ma) of ancient seep carbonates in the isotopic compilation shown in Fig. 1 (main text) and Table DR1.

A

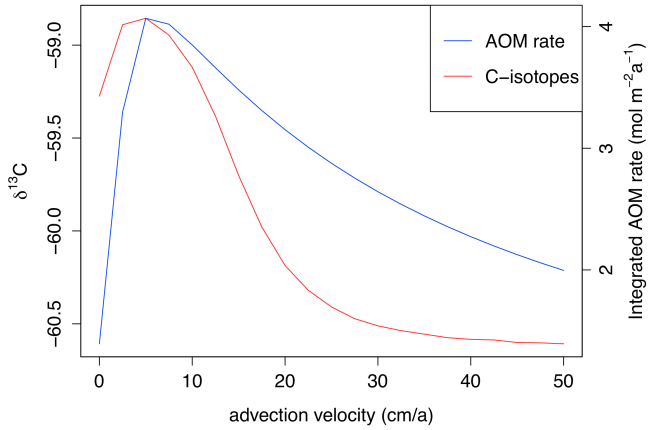

B

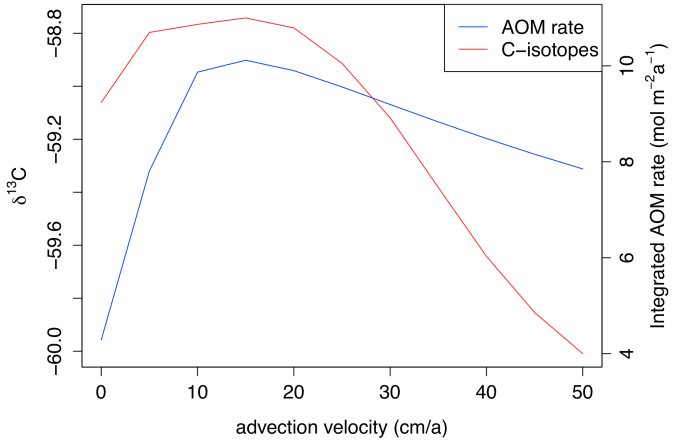

Figure DR2. AOM rate and the δ ^{13}C (PDB) of carbonates as a function of advection velocity with AOM maximum rate constants set at (A) 50, and (B) 300 mmol kg^{-1}a^{-1}.

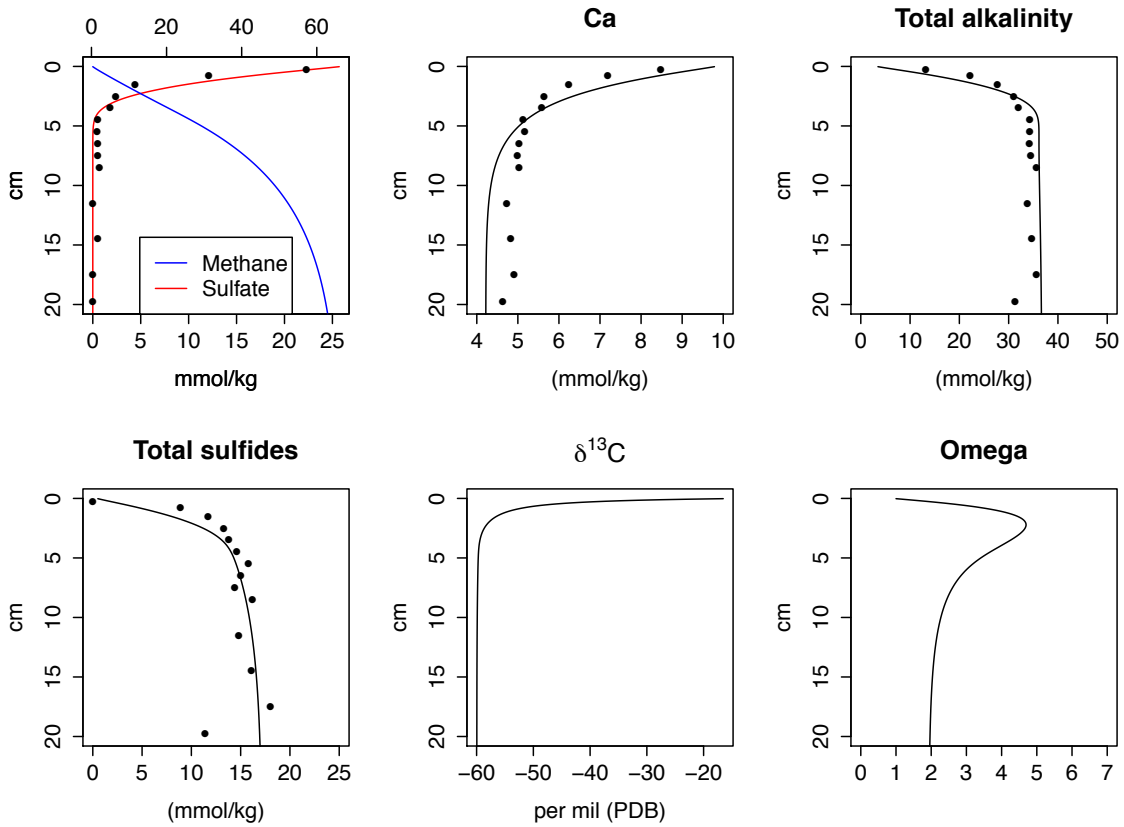

Figure DR3. Comparison of model results (solid lines) with pore water data (points) from Hydrate Ridge core SO143/114-1 (Luff et al., 2005).

Table DR1. Minimum $\delta^{13}C_{PDB}$ values of seep carbonates reported from the geological record.

Approximate Age (Ma)	Location	Minimum $\delta^{13}C$ (‰, PDB)	Reference
0.1	Offshore Russia	-49.2	Campbell et al., 2002
0.5	Central Japan	-62.3	Shibasaki and Majima, 1997
1.8	Central Japan	-55	Majima et al., 1996
2	Japan	-46	Majima et al., 2005
2	Japan	-53.2	Majima et al., 2005
2	Japan	-54.5	Majima et al., 2005
4	Washington State, USA	-33.6	Campbell, 1992
5	Japan	-58.8	Majima et al., 2005
7	Taranaki Basin, New Zealand	-40	Nyman and Nelson, 2011
8	Santa Cruz	-13.8	Aiello et al., 2001
14	N. Italy	-40	Clari et al., 1994; Peckmann et al., 1999
14	Appenines, Italy	-58	Terzi et al., 1994; Conti and Fontana, 1999
14	NE New Zealand	-51.7	Campbell and Francis, 1998
15	Japan	-23	Majima et al., 2005
23	North slope, Alaska	-69	Campbell et al., 2000
26	Heath Shale, Peru	-37.9	Kiel and Peckmann, 2007
28	Asphalt mine, Cuba	-32.2	Kiel and Peckmann, 2007
28	Columbia	-51.3	Kiel and Peckmann, 2007
28	Carpathians of Poland	-39	Bojanowski, 2007
28	Lincoln Creek Fm, WA, USA	-51	Peckmann et al., 2002
31	Juan de Fuca, WA, USA	-34.5	Geodert and Campbell, 1995
36	Whiskey Creek, WA	-36	Peckmann et al., 2003
40	Lomitos chert, Peru	-25.3	Kiel and Peckmann, 2007
50	Bulgaria	-44.8	De Boever et al., 2008
60	Panoche hills, CA	-47	Schwartz et al., 2003
76	Tepee Buttes, CO	-50	Kauffman et al., 1996
80	Hokkaido, Japan	-43.5	Jenkins et al., 2007

112	California	-24.9	Campbell et al., 2002
112	Canadian Arctic Islands (Ellef Ringes and Prince Patrick)	-50	Beauchamp et al., 1989; Beauchamp and Savard, 1992
135	California	-24.3	Campbell et al., 2002
145	Svalbard	-43	Hammer et al., 2011
150	Antarctica	-44.6	Kelly et al., 1995
150	California, USA	-43.7	Campbell et al., 2002
160	France	-26.5	Gaillard et al., 1992
190	Argentina	-33	Gomez-Pérez, 2003
215	Eastern Oregon, USA	-36	Peckmann et al., 2011
300	Namibia	-51	Himmler et al., 2008
313	France	-50	Buggisch and Krumm, 2005
350	Germany	-32	Peckmann et al., 2001
370	Morocco	-12	Peckmann et al., 2007
390	Morocco	-22	Peckmann et al., 1999b; Buggisch and Krumm, 2005; Peckmann et al., 2005
420	Morocco	-6.14	Barbieri et al., 2004; Buggisch and Krumm, 2005
635	SE Australia	-10	Kennedy et al., 2008

Table DR2. Summary of criteria used to identify Paleozoic seeps lacking carbonates with $\delta^{13}C_{PDB}$ values <-30‰.

Age (Ma)	Location	Criteria used in identification as a cold seep		Diagenetic influence on $\delta^{13}C$ values?	Reference
		Geological context, textures, fabrics	**Fossils**		
370	Morocco	Fibrous calcite cement that form isopachous rims and botryoids directly on brachiopod shells – similar textures found in other seeps. Pyrobitumen provides evidence of hydrocarbon seepage.	Dense clusters of articulated (autochthonous) *Dzieduszyckia* brachiopods, with some tubeworm fossils. Fossilized threadlike microorganisms.	Late-stage calcite filled veins crosscut banded/botryoidal cements. Original aragonitic mineralogy has been calcitized. However, most $\delta^{13}C_{PDB}$-depleted cements have $\delta^{18}O$ values close to oceanic equilibrium and distinctive from diagenetic phases.	Peckmann et al., 2007
390	Morocco	Association of the carbonate mound core with fissures and neptunian dykes, which may have provided conduits for hydrocarbon bearing fluids. Carbonates exhibit typical seep textures, consisting of clotted micrites, rim cements with botryoidal structures and stromotactis type pores. Moderate $\delta^{13}C_{PDB}$ depletion (to -22‰) make hydrocarbon oxidation likely source of carbonate alkalinity.	Dense clusters of articulated (autochthonous) bivalves and tubeworms likened to fauna from modern seeps. In contrast, host sediments are fossil poor.	Some neomorphic and vein filling dolomites reported. $\delta^{18}O_{PDB}$ values as low as -13‰, suggest post-burial recrystallization. But, carbonate cements with the lowest $\delta^{13}C_{PDB}$ values have $\delta^{18}O_{PDB}$ of -1.5‰ - suggesting preservation of original values.	Peckmann et al., 1999b; Buggisch and Krumm, 2005; Peckmann et al., 2005
420	Morocco	Localized mound (70 by 30m) of authigenic carbonate with abundant microbial fabrics hosted by a siliciclastic flysch sequence. Multiple phases of carbonate cementation and recrystallization linked to changing seep fluid chemistry. The carbonate botryoids, splayed calcite and stromactoid structures observed are common in other seeps.	Dense, localized, mono-specifc, accumulations of fully articulated *Atrypid* brachiopods. Interpreted as being preserved *insitu* and harboring chemoautotrophic symbionts. Remnant microbial mat textures comparable to mats from modern chemosynthesis based environments.	Some post-burial diagenesis indicated by alteration of brachiopod shells. However, early cavity filling carbonate cements have $\delta^{13}C_{PDB}$ between -5 to +20‰ (the heavy values recording methanogenesis); the heterogeneity indicates preservation of original signals. Carbonates with $\delta^{13}C_{PDB}$ minima used in our compilation have $\delta^{18}O_{PDB}$ values of -5‰, close to expected equilibrium values with seawater.	Barbieri et al., 2004; Buggisch and Krumm, 2005

635	SE Australia	Highly $\delta^{18}O$ enriched carbonates typical of methane seeps. Network of carbonate cemented chimneys hosted by sandstones indicates syndepositional fluid seepage.	NA	Minimal diagenetic influence on stable isotopes supported by: 1) microcrystalline nature of cement, 2) isotopic heterogeneity on millimetre scales, and 3) clay mineralogy of host sediments indicate diagenetic temperatures < 100°C.	Kennedy et al., 2008

Table DR3. Model reaction terms.

Species	Reaction term
CO_2	$((K_{-1}[H^+]+K_{-4})[HCO_3^-]) - ((K_{+1}+K_{+4}[OH^-])[CO_2])$
HCO_3^-	$((K_{+1}+K_{+4}[OH^-])[CO_2]) - ((K_{-1}[H+]+K_{-4})[HCO3-]) + ((K_{H+5}[H^+]+K_{OH-5})[CO_3^{2-}]) - ((K_{H-5}+K_{OH+5}[OH^-])[HCO_3^-]) + R_{AOM}$
CO_3^{2-}	$((K_{H-5}+K_{OH+5}[OH^-])[HCO_3^-]) - ((K_{H+5}[H^+]+K_{OH-5})[CO_3^{2-}]) - R_{carbprec}$
$^{13}CO_2$	$((K'_{-1}[H^+]+K'_{-4})[H^{13}CO_3^-]) - ((K'_{+1}+K'_{+4}[OH^-])[^{13}CO_2])$
$H^{13}CO_3^-$	$((K'_{+1}+K'_{+4}[OH^-])[^{13}CO_2]) - ((K'_{-1}[H+]+K'_{-4})[H^{13}CO_3^-]) + ((K_{H+5}[H^+]+K_{OH-5})[^{13}CO_3^{2-}]) - ((K_{H-5}+K_{OH+5}[OH^-])[H^{13}CO_3^-]) +R_{13CAOM}$
$^{13}CO_3^{2-}$	$((K_{H-5}+K_{OH+5}[OH^-])[H^{13}CO_3^-]) - ((K_{H+5}[H^+]+K_{OH-5})[^{13}CO_3^{2-}]) - R_{13Ccarbprec}$
H^+	$K_{+1}[CO_2] - K_{-1}[H^+][HCO_3^-] + K_{H-5}[HCO_3^-] - K_{H+5}[H^+][CO_3] + K_{+6} - K_{-6}[H^+][OH^-]$
OH^-	$K_{-4}[HCO_3^-] - K_{+4}[CO_2][OH^-] - K_{OH+5}[HCO_3^-][OH^-] + K_{OH-5}[CO_3^{2-}] + K_{+6}- K_{-6}[H^+][OH^-]$
HS^-	$(K_{+7}[H_2S]) - (K-_7[HS^-][H^+])$
H_2S	$(K-_7[HS^-][H^+]) - (K+7[H2S])$
Ca^{2+}	$- R_{carbprec}$
CH_4	$- R_{AOM}$
SO_4^{2-}	$- R_{AOM}$

Table DR4. Model parameter values used in the baseline simulation of pore water data from Hydrate Ridge.

Parameter	Value	Unit
Length of the simulated core	35	cm
Number of layers used in model simulation	800	
Temperature	5	°C
Salinity	34.3	PSU
Pressure	79	Bar
Background porosity at the sediment surface	0.76	
Background porosity at base of simulated profile	0.66	
Porosity depth attenuation coefficient	0.22	
Fluid velocity at sediment-water interface	30	cm a^{-1}
Kinetic constant of aragonite precipitation	0.03	mmol $kg^{-1}cm^{-3}a^{-1}$
Kinetic constant of AOM	300	mmol $kg^{-1}a^{-1}$
Diffusive boundary layer thickness	0.2	cm
Half-saturation constant methane	1	mmol kg^{-1}
Half-saturation constant sulfate	0.5	mmol kg^{-1}
Water chemistry (sediment/water interface)		
Total alkalinity	2.46	mmol kg^{-1}
pH	7.66	
Total sulfide	0.11	mmol kg^{-1}
$\delta^{13}C_{PDB}$ of seawater	0	
Calcium concentration	10.09	mmol kg^{-1}
Base of simulated column		
$\delta^{13}C_{PDB}$ of methane	-65	‰
Methane concentration	66	mmol kg^{-1}

Table DR5. Results of sensitivity tests; showing the influence of parameters other than the dissolved inorganic carbon concentration, sulfate concentration, and the carbon isotope composition of methane, on the mean $\delta^{13}C_{PDB}$ of carbonates, SMTZ depth and integrated AOM rate at seeps.

Parameter tested	Mean $\delta^{13}C_{PDB}$ of carbonates (‰)	SMTZ depth (cm)	Integrated AOM rate (mol m^{-2} a^{-1})
Temperature (°C)			
5	-58.8	1.55	12.2
19	-58.3	2.21	15.4
Pressure (bar)			
10 (~100 m depth)	-58.6	1.55	12.2
310 (~3100 m depth)	-59.2	1.55	12.2
Bottom water pH			
7	-58.2	1.55	12.2
9	-59.1	1.55	12.2
Diffusive boundary layer (mm)			
0.5	-58.7	1.64	12.4
2.5	-58.8	1.51	12.2
Methane concentration at base (mM)			
50 (saturation @3 °C, ~1000m)	-58.8	1.90	11.6
150 (saturation @20 °C, ~3000m)	-58.8	0.85	13.0
Porosity			
0.5 (set as constant)	-58.8	1.47	11.2
0.9 (set as constant)	-58.6	2.03	13.8

REFERENCES

Aiello, I.W., Garrison, R.E., Moore, J.C., Kastner, M., and Stakes, D.S., 2001, Anatomy and origin of carbonate structures in a Miocene cold seep field: Geology, v. 29, p. 1111–1114.

Aloisi, G., 2008, The calcium carbonate saturation state in cyanobacterial mats throughout Earth's history: Geochimica et Cosmochimica Acta, v. 72, p. 6037-6060.

Barbieri, R., Ori, G.G., Cavalazzi, B., 2004, A Silurian cold- seep ecosystem from the Middle Atlas, Morocco: Palaios, 19, p. 527 – 542.

Beal, E.J., House, C.H., and Orphan, V.J., 2009 Manganese- and iron-dependent marine methane oxidation: Science, v. 325, p. 184–187.

Beauchamp, B., Krouse, H.R., Harrison, J.C., Nassichuk, W.W., and Eliuk, L.S., 1989, Cretaceous cold-seep communities and methane-derived carbonates in the Canadian Arctic: Science, v. 244, p. 53–56.

Beauchamp, B., and Savard, M., 1992, Cretaceous chemosynthetic carbonate mounds in the Canadian Arctic: Palaios, v. 7, p. 434–50.

Boetius, A., et al., 2000, A marine microbial consortium apparently mediating anaerobic oxidation of methane: Nature, v. 407, p. 623–626.

Bojanowski, M.J., 2007, Oligocene cold-seep carbonates from the Carpathians and their inferred relation to gas hydrates: Facies, v. 53, p. 347-360.

Buggisch, W., and Krumm, S., 2005, Palaeozoic cold seep carbonates from Europe and North Africa - an integrated isotopic and geochemical approach: Facies, v. 51, 585-602.

Clari, P., Fornara, L., Ricci, B., and Zuppi, G.M., 1994, Methane-derived carbonates and chemosynthetic communities of Piedmont (Miocene, northern Italy): an update. Geo-Marine Letters, v. 14, 201–209.

Campbell, K.A., 1992, Recognition of a Mio–Pliocene cold seep setting from the northeast Pacific convergent margin, Washington, USA: Palaios, v. 7, p. 422–433.

Campbell, K.A., and Francis, D., 1998, Miocene methane-seep carbonates of the East Coast Basin, North Island, New Zealand: Geological Society of New Zealand Miscellaneous Publication, v. 101A.

Campbell, K.A., Aharon, P., and Marincovich Jr., L., 2000, Paleo-gas hydrates in the Arctic Ocean: evidence from Late Neogene Nuwok strata, northern Alaska: Geological Society of America Abstracts with Programs, v. 32.

Campbell, K.A., Farmer, J.D., and Des Marais, D., 2002, Ancient hydrocarbon seeps from the Mesozoic convergent margin of California: carbonate geochemistry, fluids and palaeoenvironments: Geofluids v. 2, 63–94.

Conti, S., and Fontana, D., 1999, Miocene chemoherms of the northern Appenines, Italy: Geology, v. 27, p. 927–930.

De Boever, E., Dimitrov, L., Muchez, P., and Swennen, R., 2008, The Pobiti Kamani area (Varna, NE Bulgaria) — study of a well-preserved paleo-seep system. Review of the Bulgarian Geological Society, v. 69, 61-68.

Gaillard, C., Rio, M., Rolin, Y., and Roux, M., 1992, Fossil chemosynthetic communities

related to vents or seeps in sedimentary basins: the pseudobioherms of southeastern France compared to other world examples: Palaios, v. 7, p. 451–65.

Goedert, J.L., and Campbell, K.A., 1995, An Early Oligocene chemosynthetic community from the Makah Formation, northwestern Olympic peninsula: The Veliger, v. 38, p. 22–29.

Gomez-Pérez, I., 2003, An Early Jurassic deep-water stromatolitic bioherm related to possible methane seepage (Los Molles Formation, Neuquén, Argentina): Palaeogeography, Palaeoclimatology, Palaeoecology, v. 201, p. 21–49.

Hammer, Ø. et al., 2011, Hydrocarbon seeps from close to the Jurassic–Cretaceous boundary, Svalbard: Palaeogeography, Palaeoclimatology, Palaeoecology, v. 306, p. 15-26.

Himmler, T., Freiwald, A., Stollhofen, H., and Peckmann, J., 2008, Late Carboniferous hydrocarbon-seep carbonates from the glaciomarine Dwyka Group, southern Namibia: Palaeogeography, Palaeoclimatology, Palaeoecology, v. 257, p. 185–197.

Hoehler, T.M., Alperin, M.J., Albert, D.B. and Martens, C.S., 1994, Field and laboratory studies of methane oxidation in an anoxic marine sediment: Evidence for a methanogenic-sulfate reducer consortium: Global Biogeochemical Cycles, v. 8, p. 451-463.

Jenkins, R., Kaim, A., Hikida, Y., and Tanabe, K., 2007, Methane-flux-dependent lateral faunal changes in a Late Cretaceous chemosymbiotic assemblage from Nakagawa area of Hokkaido, Japan: Geobiology, v. 5, p. 127–140.

Kauffman, E.G., Arthur, M.A., Howe, B. and Scholle, P.A., 1996, Widespread venting of methane-rich fluids in Late Cretaceous (Campanian) submarine springs (Tepee Buttes), Western Interior Seaway, USA: Geology, v. 24, p. 799–802.

Kelly, S.R.A., Ditchfield, P.W., Doubleday, P.A., and Marshall, J.D.A., 1995, Late Jurassic methane-seep limestone from the fore-arc basin of Alexander Island, Antarctica: Journal of Sedimentary Research, v. A65, 274–82.

Kennedy, M., Mrofka, D., and von der Borch, C., 2008, Snowball Earth termination by destabilization of equatorial permafrost methane clathrate: Nature, v. 453, p. 642-645.

Kiel, S., and Peckmann, J., 2007, Chemosymbiotic bivalves and stable carbon isotopes indicate hydrocarbon seepage at four unusual Cenozoic fossil localities: Lethaia, v. 40, p. 345–357.

Lavigne, H., and Gattuso, J. P., 2012, *seacarb: Seawater carbonate chemistry with R*, (R package version 2.4.3).

Luff, R., Greinert, J., Wallmann, K., Klaucke, I., and Suess, E., 2005, Simulation of long-term feedbacks from authigenic carbonate crust formation at cold vent sites: Chemical Geology, v. 216, p. 157–174.

Majima, R., Tate, Y., and Shibasaki, T., 1996, In situ fossil chemosynthetic community found from the lower Pleistocene Kazusa Group, Yokohama City, central Japan: Fossils, v. 61, p. 47–57.

Majima, R., Nobuhara, T., and Kitazaki, T., 2005, Review of fossil chemosynthetic assemblages in Japan: Palaeogeography, Palaeoclimatology, Palaeogeography, v. 227, p. 86-123.

Millero, F.J., 1995, Thermodynamics of the carbon dioxide system in the oceans: Geochimica et Cosmochimica Acta, v. 59, p. 661-677.

Nyman, S.L., and Nelson, C.S., 2011,The place of tubular concretions in hydrocarbon cold seep systems: Late Miocene Urenui Formation, Taranaki Basin, New Zealand: American Association of Petroleum Geologists Bulletin, v. 95, p. 1495-1524.

Peckmann, J., et al., 1999, Cold seep deposits of Beauvoisin (Oxfordian, southeastern France) and Marmorito (Miocene, northern Italy): microbially induced authigenic carbonates: International Journal of Earth Sciences, v. 88, 60–75.

Peckmann, J., Walliser, O.H., Riegel, W., and Reitner, J., 1999b, Signatures of hydrocarbon venting in a Middle Devonian carbonate mound (Hollard Mound) at the Hamar Laghdad (Antiatlas, Morocco): Facies, v. 40, p. 281–296.

Peckmann, J., Gischler, E., Oschmann, W., and Reitner, J., 2001, An Early Carboniferous seep community and hydrocarbon-derived carbonates from the Harz Mountains, Germany: Geology, v. 29, p. 271–274.

Peckmann, J., Goedert, J.L., Thiel, V., Michaelis, W., and Reitner, J.A., 2002, comprehensive approach to the study of methane-seep deposits from the Lincoln Creek Formation, western Washington State, USA: Sedimentology, v. 49, p. 855–873.

Peckmann, J., Little, C.T.S., Gill, F., and Reitner, J., 2005, Worm tube fossils from the Hollard Mound hydrocarbon-seep deposit, Middle Devonian, Morocco: Paleozoic seep-related vestimentiferans?: Palaeogeography, Palaeoclimatology, Palaeoecology, v. 227, p. 242-257.

Peckmann, J., Campbell, K.A., Walliser, O.H., Reitner, J., 2007, A Late Devonian hydrocarbon-seep deposit dominated by Dimerelloid Brachiopods, Morocco: Palaios, v. 22, 114-122.

Peckmann, J., Kiel, S., Sandy, M.R., Taylor, D.G., and Goedert, J.L., 2011, Mass Occurrences of the Brachiopod Halorella in Late Triassic Methane-Seep Deposits, Eastern Oregon: Journal of Geology, v. 119, p. 207-220.

Peckmann, J., Goedert, J.L., Heinrichs, T., Hoefs, J., and Reitner, J., 2003, The Late Eocene 'Whiskey Creek' methane-seep deposit (western Washington State): Part II. Petrology, stable isotopes, and biogeochemistry: Facies, v. 48, p. 241–254.

R Development Core Team, *R: A Language and Environment for Statistical Computing* (R Foundation for Statistical Computing, Vienna, Austria 2011).

Regnier, P. et al., 2011, Quantitative analysis of anaerobic oxidation of methane (AOM) in marine sediments: A modeling perspective: Earth Science Reviews, v. 106, 105-130.

Schwartz, H., Sample, J., Weberling, K.D., Minisini, D., and Moore, J.C., 2003, An ancient linked fluid migration system: cold-seep deposits and sandstone intrusions in the Panoche Hills California, USA: Geo-Marine Letters, v. 23, p. 340–350.

Shibasaki, T., and Majima R.A., 1997, fossil chemosynthetic community from outer shelf environment of the Middle Pleistocene Kakino- kidai Formation, Kazusa Group in Boso Peninsula, Chiba Prefecture, central Japan: Journal of the Geological Society of Japan, v. 103, p. 1065–80.

Soetaert, K., and Meysman, F., 2009, ReacTran: Reactive transport modelling in 1D, 2D and 3D. (R package version 1.1).

Soetaert, K., Petzoldt, T., and Meysman, F., 2010, marelac: Tools for Aquatic Sciences (R package version 2.1).

Terzi, C., Aharon, P., Ricci Lucchi, F., and Vai, G.B., 1994, Petrography and stable isotope aspects of cold-vent activity imprinted on Miocene-age "calcari a Lucina" from Tuscan and Romagna Appenines, Italy: Geomarine Letters, v. 14, p. 177–184.

Urbanek, S., 2009, multicore: Parallel processing of R code on machines with multiple cores or CPUs (R package version 0.1-4).

Wegener, G., and Boetius, A., 2009, An experimental study on short-term changes in the anaerobic oxidation of methane in response to varying methane and sulfate fluxes: Biogeosciences, v. 6, p. 867-876.

Zeebe, R.E., and Wolf-Gladrow, D., 2001, CO_2 in seawater: equilibrium, kinetics, isotopes: Amsterdam, Elsevier, 345 p.